Design and comparative analysis of a control strategy approach implemented to hybrid energy storage system based electric vehicle

Raghavaiah Katuri[1,*], Srinivasarao Gorantla

Department of Electrical and Electronics Engineering,
Vignan's Foundation for Science, Technology and Research, Vadlamudi, Guntur 522213, Andhra Pradesh, India

rk_eeep@ vignanuniversity.org

ABSTRACT. The usages of electric vehicles (EVs) are increased drastically than IC engine based vehicles in order to protect the environment. During peak power requirement, to diminish the burden on the battery, Hybrid Energy Storage System (HESS) is developed by combining battery with ultracapacitor (UC). HESS based electric vehicles always give better results than the only battery-fed electric vehicle. The transition between the energy sources according to the driving conditions is the key obstacle associated with HESS based EVs. The key objective of this work is to realize a new controller control strategy, to switch the battery and UC according to the electric vehicle requirement. Total four math functions are considered and programmed individually corresponding to the speed of an electric motor called as Math Function Based (MFB) controller, thereafter the designed MFB has combined with conventional controllers formed a new hybrid controller for switching the energy sources according to the speed of an electric motor. In this work battery gets charged from the solar power during sunlight available timings, in the same way, discharges the same amount of power to the electric motor. A comparative analysis is done between two hybrid controllers named as MFB with PID and MFB with PI, based on different factors. All modes MATLAB/Simulation results are plotted and discussed.

RÉSUMÉ. Les usages des véhicules électriques (EVs) sont considérablement augmentés par rapport aux véhicules à moteur thermique afin de protéger l'environnement.Lors des pics de consommation, afin de réduire la charge de la batterie, le système de stockage d'énergie hybride (HESS) est développé en combinant la batterie avec un ultra-condensateur (UC).Les véhicules électriques à base de HESS donnent toujours de meilleurs résultats que le seul véhicule électrique alimenté par batterie. La transition entre les sources d'énergie en fonction des conditions de conduite est le principal obstacle associé aux véhicules électriques à base de HESS.L'objectif principal de ce travail est de mettre au point une nouvelle stratégie de contrôle du contrôleur, consistant à commuter la batterie et l'UC en fonction des besoins du véhicule électrique.Quatre fonctions mathématiques au total sont considérées et programmées individuellement pour correspondre à la vitesse d'un moteur électrique appelé contrôleur à

fonction mathématique (MFB),ensuite, le MFB conçu a été associé à des contrôleurs conventionnels pour former un nouveau contrôleur hybride permettant de commuter les sources d'énergie en fonction de la vitesse d'un moteur électrique.Dans ce travail, la batterie se charge de l'énergie solaire pendant les périodes de lumière du soleil. De la même manière, la puissance identiaue est fournie au moteur électrique. Une analyse comparative est effectuée entre deux contrôleurs hybrides nommés MFB avec PID et MFB avec PI, en fonction de différents facteurs.Les résultatsde tous les modes MATLAB / simulation sont tracés et discutés.

1. Introduction

Anciently Battery is used to propel the electric vehicle in all road conditions like starting, running and transient period of the vehicle. A hybrid flywheel/battery system is used for storing the braking energy and it can be utilized during peak loads of electric vehicles in order to reduce the burden on the battery (Lustenader *et al*., 1977). Embedded energy storage system has been made with Fuel cell and UC, a polynomial method is used to split the energy between two sources according to the energetic request of HEV. A fuel cell is used for meeting the average power and UC is used for fluctuating for the requirement of HEV (Tani *et al.*, 2013). The energy management between high energy density device battery and high power density device UC has been made with the controller for emergency starting of an IC engine to save the life of the rich energy device. In the designed power source UC gets charged from the battery very quickly and discharges energy at the same rate which makes the IC engine proper starting (Averbukh *et al*., 2015).

The HESS has been developed for EV/HEV application in that, energy management is the main issue to split the energy between battery and UC. Energy management strategy has developed with an adaptive FLC to manage the power splitting between the two sources. The designed adaptive fuzzy logic controller enhances the overall system efficiency by sharing the transient power to the UC and average power to the battery (Yin *et al*., 2016). To make proper energy management between the battery and UC 2- real-time controllers are developed for finest current sharing between UC and battery in EV application. One of the controller is developed based on Karush–Kuhn–Tucker conditions by solving the formulated optimization problem, which makes the right current splitting of HESS. The second controller is developed based on neural network and that is termed as an intelligent controller. Based on the current sharing of energy sources controller performance has been evaluated (Shen *et al*., 2016). With a variable rate–limit function an adaptive energy management control has been designed for energy storage system. The designed energy sharing controller is saving the life of the main source of the Energy Storage

System (ESS). Steady state power can be supplied by the main source and aggressive power during the transient period can be supplied by the auxiliary source. Here the auxiliary source is capable of charging and discharging of energy at very less time though it has low energy density property (Wu *et al.*, 2015).

In hybrid storage technology, battery and supercapacitor (SCAP) are combined, implemented a control technique to share the energy between the sources as per HEV demands. Here SCAP is used to meet the peak power requirement whereas battery is for normal power demands. These works focus on that how the SCAP is behaving during different load conditions of HEV. Based on the behavior of an HEV required energy management strategy is designed and implanted with a reduced scaled parameter in order to reduce the build cost. (Camara *et al.*, 2008). HESS has been implemented with UC and battery and the bidirectional DC-DC converter is used with low power for the design of the controller for proper power management of the input sources. The HESS is operated in four modes within its power limit for proper power split between UC and battery (Xiang *et al.*, 2014). In this, a novel HESS is designed with battery and UC. The traditional HESS has integrated the source through high rating DC-DC converters to the vehicle, whereas in proposed HESS; sources are connected through low rating DC-DC converters to the vehicle. An interface is created between battery and UC in order to meet the peak power requirement of the vehicle. The relative load profile is created to the battery for supplying the power directly to the vehicle even UC voltage value drops to a low value. The battery is not used here to charge directly from the regenerative braking which will reduce the charging and discharging burden (Cao *et al.*, 2012). EMS is implemented based on the numerical methods for HEVs. This controller does not need the previous driving data and the overall controller can be achieved according to the driver requirements and is formulated as a nonlinear receding horizon control problem (Zhang *et al.*, 2015). Now day's electric vehicles are more popular in usage, but they are lagged with some drawbacks in that storage of energy is the main problem and lack of charging stations availability. By constructing several charging stations at thickly populated areas recharging of batteries can be avoided. On another way, electric vehicles are constructed with a solar panel to recharge the battery during sunlight available times. Generally, solar-powered electric vehicles are more useful than only battery-powered electric vehicles (Kuperman *et al.*, 2011). In this work, solar power can support the battery-powered EV. The balancing of a battery can be achieved corresponding to the SOC of the battery, and the battery gets charged form the solar panel if the solar power was available. Suppose if solar power is not available then the battery can discharge its energy to the motor until its state of charge value reaches the specified value (Song *et al.*, 2014). Generally, maximum numbers of electric vehicles are fed with its own solar panel to charge the battery during sunlight available timings. And also solar-powered charging stations also are installed at some places to charging the battery if vehicle own solar power is not sufficient. If connected batteries are fully charged then the power generated by the solar power station can be transferred to the utility grid otherwise generated power cannot be useful, this power transmission can be done based on the maximum power point tracking (Sadagopan *et al.*, 2014). Releasing of

Greenhouse gases is the major problem with the conventional transportation system. In order to overcome those emission problems, conventional vehicles are replaced with eco-friendly vehicles like electric vehicles. In this work design of electric vehicle have been done to meet maximum environment conditions (Manivannan *et al*., 2016). This work mainly focusing on, designing of a new control strategy to switch the battery and UC as per the requirement of the electric vehicle in an accurate way. Here solar panel is considered to charge the battery during sunlight available timings.

2. Proposed system model

Figure 1 illustrates that the proposed HESS of an electric vehicle containing two sources in that battery is the main sources and UC will act as a supporting source. Generally, the battery can supply the base power on the other hand UC can supply the peak power to the electric motor. The solar panel can generate the power which is required to charge the battery as well as the input of Unidirectional converter (UDC). Here control switches are connected to the solar panel, UDC and battery, depending upon the control switches action the battery charging and discharging actions can take place. Two controllers are connected for obtaining the required pulse signals to the switches which are present in the unidirectional converter (UDC) as well as a Bidirectional converter (BDC) named as MFB and conventional controller.
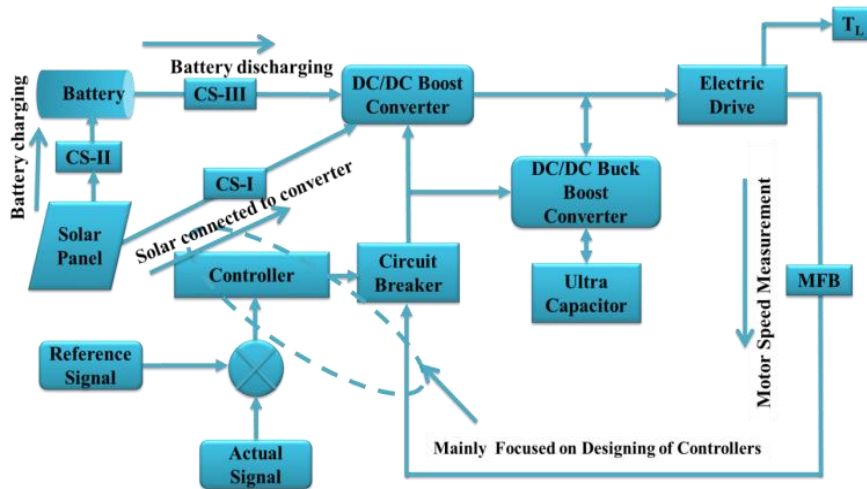

Figure 1. The Block Diagram Model of HESS with proposed control strategy approach
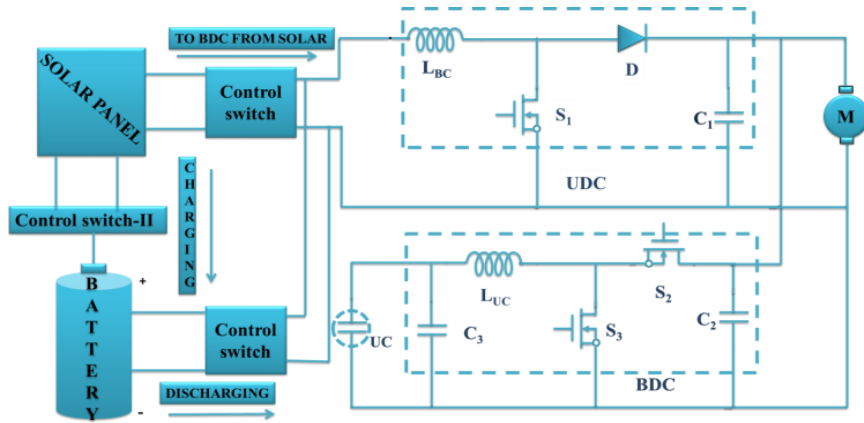
Figure 2. Main circuit model with DC-DC converters

Figure 2 contains mainly battery, UC, UDC, and BDC. Here BDC can perform either boost operation or buck operation. During UC discharging time BDC working under boost mode on other hand behaves as a buck converter during charging of UC. But UDC performs only boost mode operation to discharge the battery. The whole circuit contains total three switches to perform the required operation of an electric motor, in that switch S1 belongs to UDC and remain two switches S2, S3 related to BDC to perform buck and boost converter operation. One solar panel also connected here to charge the battery. Here the battery charging and discharging conditions are depending upon the SOC of the battery as well the control switches connected among battery, solar panel, and UDC.

3. Description of controllers used in the proposed model

In this work mainly two controllers are used to achieve the proposed control scheme. In that, the conventional controller is the first one and the second one is Math function based controller. The combination of selected two controller forms a new controller to switch the energy sources of HESS according to the speed of an electric motor.

3.1. MFB controller

Among all controllers, MFB controller performs an important role during the generation of controlled signals to the particular converter corresponding to the speed of an electric motor. The conventional controller generates the pulse signals to the converter by comparing the reference signal with actual signal, thereafter this error signal can be compared with the MFB produced signal and corresponding output

signals are applied to the converter switches. The converter applied signals are always corresponding to the speed of an electric motor, which can be controlled by the MFB controller. The designed MFB controller produces four math function signals corresponding to the particular mode of operation. Math function U1 only is in enable state during mode-1 operation, in the same way, U1, U2 are in enable state in mode-2 and during mode-3 operation, only U3 is in enable condition, finally, in mode-4 math function U4 only in ON state, remaining all math functions are in disable state. All those disable and enable states of the MFB controller's leads to produce the controlled switching signals according to the speed of an electric motor. Finally, the MFB plus PI/PID makes the smooth switching of sources present in HESS. Here U1, U2, U3, and U4 are the generated outputs of MBF controller.
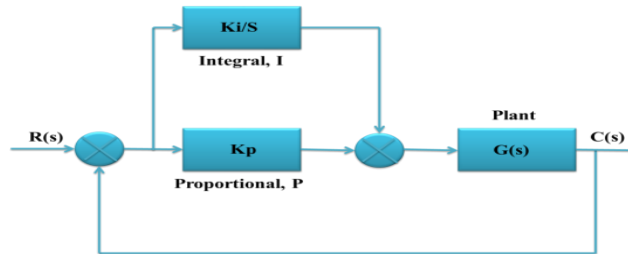
3.2. PI controller

Figure 3. PI controller block diagram

$$C(s) = K_p e + K_I \int e dt \qquad (1)$$

(a) It increases the rise time.
(b) It reduces bandwidth.
(c) It reduces the stability of the system.
(d) It increases the damping ratio, ξ and hence reduces peak overshoot.
(e) It eliminates steady-state error between input and output and hence has very high steady-state accuracy.
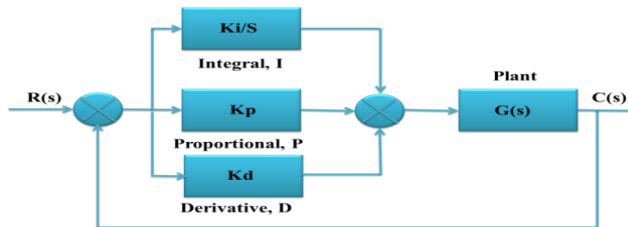
3.3. PID controller

Figure 4. PID controller block diagram

The generalized equation of representing the PID controller is

$$C(s) = K_p e + K_I \int e\,dt + K_d \frac{de}{dt} \qquad (2)$$

(a) It reduces the rise time.
(b) It increases bandwidth.
(c) It amplifies noise and hence reduces the signal to noise ratio.
(d) It increases the damping ratio, ξ and hence reduces peak overshoot.
(e) It eliminates steady-state error between input and output and hence has very high steady-state accuracy.

4. Mathematical modelling of HESS

4.1. Battery model
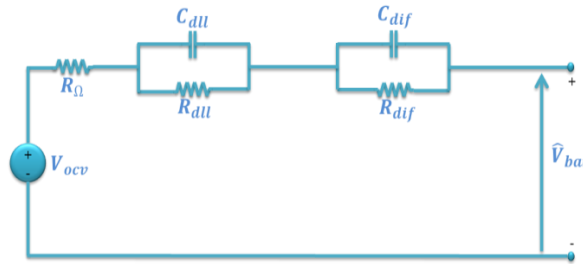
Figure 5. A dynamical model of a battery

Figure 5 shows that the dynamical model of the battery, where the terminal voltage is a function of time and is finding from three components.

$$f_1(V_t, i_l, i) = E_0 - \frac{KQi_l}{Q - V_t} - \frac{KQV_t}{Q - V_t} + E.\exp(-D.V_t) \qquad (3)$$

$$f_1(V_t, i_l, i) = E_0 - \frac{KQi_l}{V_t + 0.1Q} - \frac{KQV_t}{Q - V_t} + E.\exp(-D.V_t) \qquad (4)$$

Where E_0= constant voltage (V)

$$SOC = 100\left(1 - \frac{1}{Q}\int_0^t i(t)\,dt\right) \qquad (5)$$

i=battery current
Q=Capacity of the battery (Ah)
V_t =Extracted voltage (V)
E=Exponential voltage (V)
i_l=Low frequency current dynamics (A)
K=Polarization resistance (Ohms)

D=Exponential capacity (Ah-1)

4.2. Ultracapacitor model

Figure 6. Equivalent electrical model of UC

Figure 6 representing that the equivalent electrical model of UC. The voltage state of UC for RC is given by stern-Tafel model of the UC is the most popular model and the equations of this model can be written as

$$V = \frac{NN_sQX2}{NN_pN^2\varepsilon\varepsilon 0A} + \frac{NN_s2RT}{F}\alpha \tag{6}$$

$$-i(t) = Ai_0 \exp\left(\frac{\alpha F\left(\frac{V}{N_s} - \frac{V_{max}}{N_s} - \Delta V\right)}{RT}\right) \tag{7}$$

$$SOC = \frac{Qinit - \int_0^t i(\tau)d\tau}{QT} \times 100 \tag{8}$$

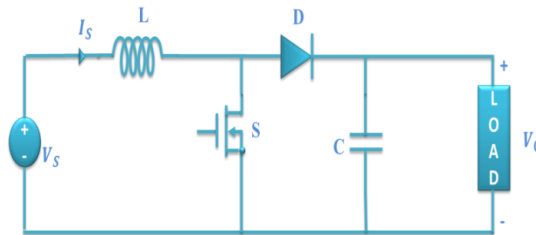### 4.3. Unidirectional converter modelling

Figure 7. Unidirectional converter model

Figure 7 represents DC-DC Converter (boost), and the state space expression for the DC-DC converter (boost) during switch is in ON condition.

The generalized equation of UDC converter can be written as;

$$V = L\frac{di}{dt} \tag{9}$$

$$i = \frac{1}{L}\int_0^t V dt + i_0 \tag{10}$$

If the switch is in ON condition

$$i_{pk} = \frac{(V_o - V_i)T_{on}}{L} \tag{11}$$

$$\Delta i = \frac{(V_o - VT_{mos})T_{on}}{L} \tag{12}$$

If the switch is in OFF condition

$$i_0 = i_{pk} = \frac{(V_o - V_i + V_D)T_{off}}{L} \tag{13}$$

or

$$\Delta i = \frac{(V_o - V_i + V_D)T_{off}}{L} \tag{14}$$

V_D =Diode across voltage drop, V_{mos} = voltage drop across MOSFET

To find the V_o value equate the Δi then,

$$V_o = \frac{V_i - V_{mos}*\delta}{1 - \delta} - V_D \tag{15}$$

After neglecting the losses at MOSFET and Diode, the above equation becomes

$$V_o = \frac{V_i}{1 - \delta} \tag{16}$$

Using the above equation (16) input voltage of the converter step up to a required voltage level by changing the duty cycle.
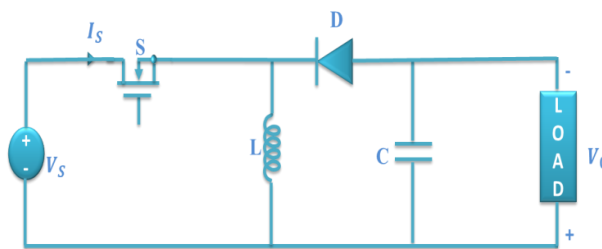
4.4. Bidirectional converter modeling

Figure 8. Bidirectional converter model

The equation for the rate of change of inductor current is given as

$$\frac{dI_L}{dt} = \frac{V_i}{L} \tag{17}$$

ON state end rewrote equation becomes

$$\Delta I_{Lon} = \int_0^{\delta T} dIL = \int_0^{\delta T} \frac{V_i}{L} dt = \frac{V_i \delta T}{L} \qquad (18)$$

The equation for IL can be written as

$$\frac{dIL}{dt} = \frac{V_0}{L} \qquad (19)$$

Therefore, the variation of I_L in the off-period is,

$$\Delta I_{Loff} = \int_0^{(1-\delta)T} dIL = \int_0^{(1-\delta)T} \frac{V_0}{L} dt = \frac{V_0(1-\delta)T}{L} \qquad (20)$$

It is obvious that the sum of variations in IL for on-state and off-state should be zero. Hence

$$\Delta I_{Lon} + \Delta I_{Loff} = 0 \qquad (21)$$

Substituting the equations of ΔI_{Lon} and ΔI_{Loff}

$$\Delta I_{Lon} + \Delta I_{Loff} = \frac{V_i \delta T}{L} + \frac{V_0(1-\delta)T}{L} = 0 \qquad (22)$$

This can be written as,

$$\frac{V_0}{V_i} = \frac{\delta}{\delta - 1} \qquad (23)$$

And

$$\delta = \frac{V_0}{V_0 - V_i} \qquad (24)$$

5. PV array mathematical modeling

Numbers of cells are connected in series and parallel to form a PV module and a number of modules are allied in series and parallel to produce the required output. Using Si-based photovoltaic modules the PV system converts only 15% of solar energy into electricity. Ideal solar PV cell is demonstrated by a current source and an inverted diode coupled in parallel to it as shown in Figure 9.

Two key parameters as short-circuit current (I_{sc}) and open circuit voltage that is frequently used to characterize a PV cell. By short-circuiting the terminals of the cell the photon generated current as shown in Figure 3(b), flows out of the cell called as a short circuit current (I_{sc}). Thus, we can say that $I_{cell} = I_{sc}$ as the current I_{cell} is flowing in a single series circuit. As the terminals are short-circuited then the voltage across the circuit is equal to zero i.e $V_{oc} = 0$ and the short-circuit current is the PV cell load current (or the output current which is very maximum as equal to that of the current source or photovoltaic photon generated current i.e. $I_{cell} = I_{sc} = I_m$Similarly,

when the terminals are open circuited i.e. no load and nothing is connected as represented in 9 (c), the load current of a PV cell becomes zero. And the load voltage of a PV cell is equal to the maximum applied source voltage or open circuit voltage i.e. ($V_m = V_{oc}$).
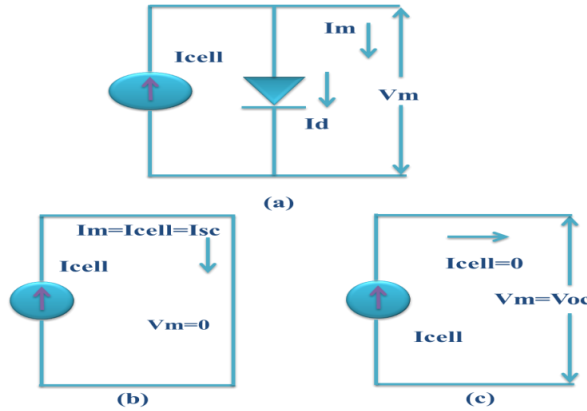

Figure 9. (a) PV cell equivalent circuit, (b) PV cell at short circuit condition (c) PV cell at open circuit condition

The PV cell output current can found by applying KVL to circuit 9(a),

$$I_m = I_{cell} - I_d \tag{25}$$

The current through diode can be represented with bellow equation

$$I_d = I_{rscell}\left[e^{\left(\frac{QV}{KT_{ap}}\right) - 1}\right] \tag{26}$$

By replacing Id in Equation 26, it gives the current-voltage relationship of the PV cell as shown below

$$I_m = I_{cell} - I_{rscell}\left[e^{\left(\frac{QV}{KT_{ap}}\right) - 1}\right] \tag{27}$$

The diode reverse saturation current (I_{rscell}) is constant under the constant temperature and irradiance that is calculated by the open circuit condition of PV cell as illustrated in Figure 9(b). From the Equation (27) it is observed that $I_m = 0$ and solve for I_{rscell}

$$I_{rscell} = \frac{I_{cell}}{\left[e^{\left(\frac{QV}{KT_{ap}}\right) - 1}\right]} \tag{28}$$

The photon generated current is directly proportional to the irradiance and temperature, whereas the voltage is directly proportional to the irradiance and inversely proportional to the temperature. The value of ISCR is provided by the manufacturer datasheet at STC (standard test condition). At STC, the working temperature and irradiance are 25 C and 1000 W/m respectively.

In the present work, the standard PV array has taken and generated the power with different temperatures and irradiance values. Thereafter using DC-DC solar panel voltage is changed according to the electric vehicle requirement. Here tree control switches are connected to the solar panel, battery, and UDC. The SOC of the battery and the output voltage of the solar panel will decide the control switches action.

6. Modes of operation of converter model

For better understanding, the proposed model circuit with a new control strategy overall circuit can be divided into four subcircuits corresponding to the speed of an electric motor. In each mode motor carries different loads like a heavy load, slightly more than rated load, rated load, no load or light load condition. All modes operation explains with neat sketches in this section.

6.1. Mode-I operation

During mode-I operation a heavy load is applied to the motor and total power can be supplied by the UC only. That means entire power flow can be from UC to motor only which means the controlled signals are produced to only switch S3 and there are no controlled signals are produced to the UDC. During a heavy load condition motor requires more than average power, so in order to reduce the burden on the main power source UC can supply entire peak power to the electric motor with that the battery charging and discharging numbers reduces which leads to improving the battery life. Here solar panel has been connected with that battery gets charged during sunlight available timings and discharges the same amount of energy to the motor when it required. Here three control switches are connected among battery, solar panel and UDC to decide the battery charging and discharging conditions based on the SOC of battery and output voltage generated by the solar panel.
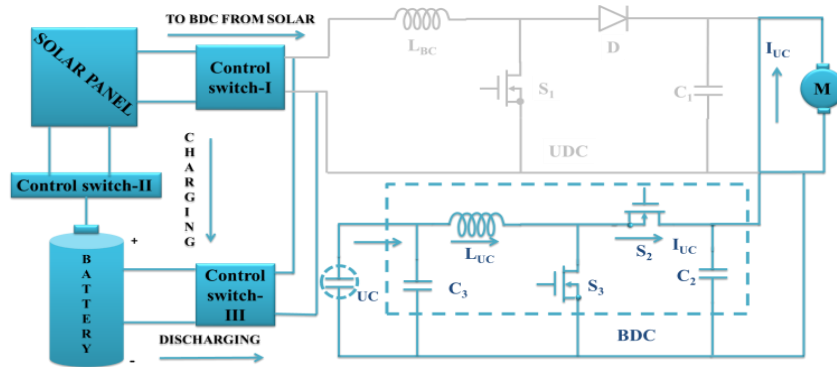
Figure 10. Main circuit model with DC-DC converters during mode-I operation

6.2. Mode-II operation

In mode-II, slightly more than rated load is applied to the electric motor and the switches S1, S3 are in the active state, another switch S2 is in disable state. The battery, as well as UC, together meet load requirement. During this mode of operation, the peak power burden on the battery can be reduced by the auxiliary source UC. So the controlled signals are produced to BDC as well as UDC working under boost mode. Here solar panel has been connected with that battery gets charged during sunlight available timings and discharges the same amount of energy to the motor when it required. Here three control switches are connected among battery, solar panel and UDC to decide the battery charging and discharging conditions based on the SOC of battery and output voltage generated by the solar panel.
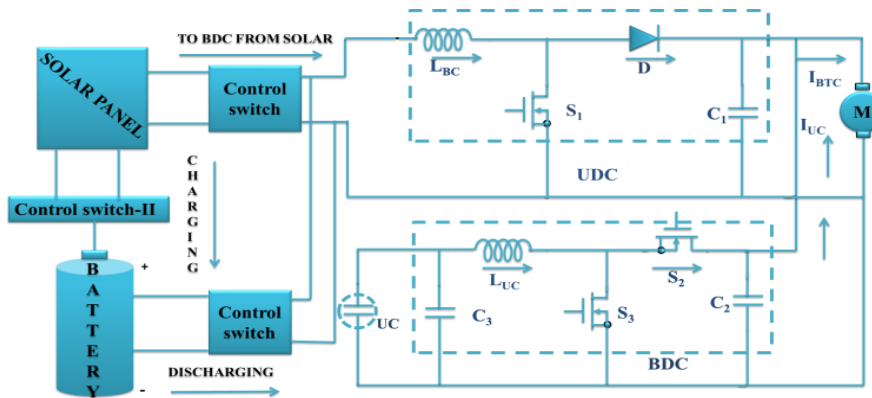

Figure 11. Main circuit model with DC-DC converters during mode-II operation

6.3. Mode-III operation

This mode is related to the rated load on the electric motor, in this switch S1 is in ON position and remain two swathes are in OFF position. During rated load condition motor draws average power only, which can be supplied by the battery itself. So the controlled signals are produced to only UDC working as a boost converter and there are no pulse signals to the BDC which indicates that this mode does not require any support from the auxiliary source. The total power flows from the battery to electric motor. Here solar panel has been connected with that battery gets charged during sunlight available timings and discharges the same amount of energy to the motor when it required. Here three control switches are connected among battery, solar panel and UDC to decide the battery charging and discharging conditions based on the SOC of battery and output voltage generated by the solar panel.
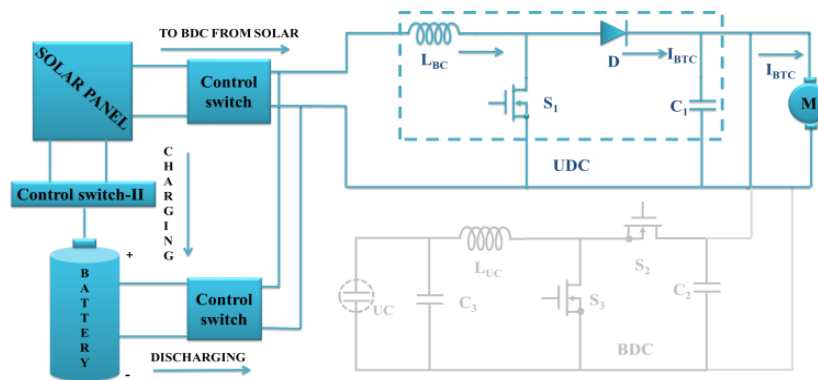

Figure 12. Main circuit model with DC-DC converters during mode-III operation

6.4. Mode-IV operation

During this mode motor is free from load or light load is applied. So switches S1, S2 are in active state and another switch S3 is in disable state. During this mode of operation, the battery can supply the required power of electric motor as well as UC for charging. The power can flow from battery to electric motor as well UC. The pulse signals are produced to UDC (boost mode) as well as BDC (buck mode). Here solar panel has been connected with that battery gets charged during sunlight available timings and discharges the same amount of energy to the motor when it required. Here three control switches are connected among battery, solar panel and UDC to decide the battery charging and discharging conditions based on the SOC of battery and output voltage generated by the solar panel.
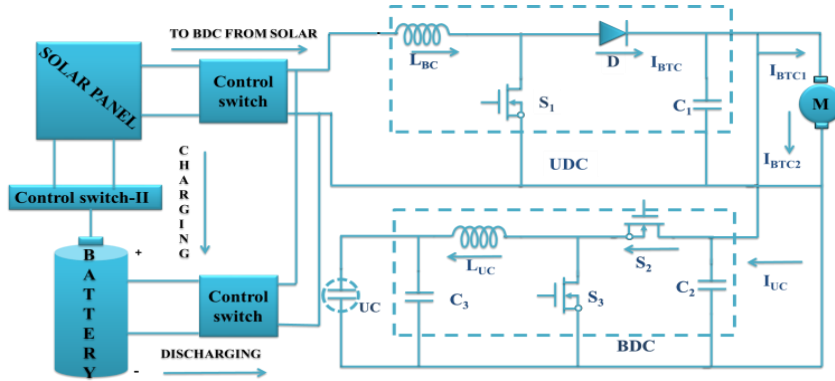
Figure 13. Main circuit model with DC-DC converters during mode-IV operation

7. Proposed model control strategy

The designed control strategy is used to switch the energy sources mainly corresponding to the speed of an electric motor. The MFB controller has designed thereafter combined with a conventional controller, formed a new hybrid controller and applied to the electric motor for a smooth transition of energy sources. Among all the controllers, MFB plays a key for applying the required pulse signal to the particular converter switch. This entire phenomenon can be illustrated with below flow chart figure 14.
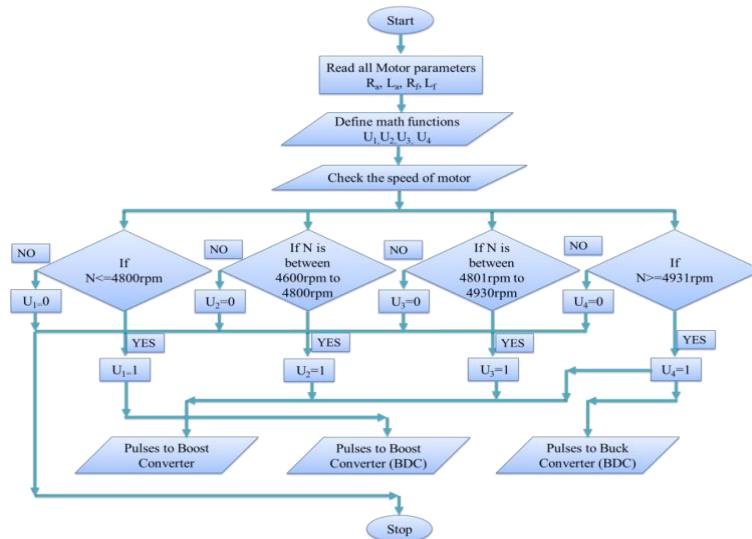

Figure 14. Developed control technique represented with the flowchart

(1) With a heavy load and starting of electric motor total power can be supplied by the UC only. The MFB controller generates out signal as 1 for math function U1 and also generates an output signal as 0 for remain math functions U2, U3, U4 corresponding to the speed of an electric motor. In this mode, the motor speed will be ≤4800 rpm and the BDC will be in operation which is connected at UC end. Finally, the designed MFB combined with other controller initiates to produce the controlled pulse signals to a particular converter.

(2) If slightly more than rated load is applied to an electric motor due to which motor speed is maintained between 4600 rpm to 4800 rpm. The MBF controller produces output signals as 1 for math functions U1, U2 and generates signals as 0 for remain math functions U3, U4 corresponding to the speed of an electric motor. Finally, controlled signals required by the converters can be generated by the designed MFB combined with another controller. UDC and BDC, both are an in-active state, under boost mode. In this mode of operation, UC reduces the burden on the battery by sharing the transient power requirement of the load.

(3) During this mode of operation rated load is applied to the electric motor, which leads to drawing average power by an electric motor. So batteries can delivery total power required by the load. Due to rated load, motor maintains a speed between 4801 rpm to 4930 rpm. The output pulse signal of the designed MFB generates as 1 for math function U3 and generates as 0 for remaining math functions U1, U2, U4 according to the speed of an electric motor. The designed MFB combined with other controller generates a controlled pulse signal to the UDC which will work under boost mode.

(4) During no load or light load condition, the battery is capable to deliver extra power to the load which is used to charge the UC. The output pulse signals of MBF controller generates as 1 for U4 and generates as 0 for U1, U2, and U3 according to the speed of an electric motor. The speed of motor maintained as >4931 rpm. The pulse signals are produced to BDC (buck mode) as well as UDC (boost mode).

Figure 15 (a), (b), (c) representing that how the control pulse signals are producing corresponding to the speed of an electric motor. Here the pulse signals are produced by the FLC and can be controlled by the MFB controller corresponding the speed of the electric motor which initiates the switching action between battery and UC. The pulse signals are producing the particular switch like based on bellow approach.

Pulse signal to switch S1: If MFB produces U2 or U3 or U4 then the pulse signal produced by the FLC can be applied to switch S1 to initiate the operation of UDC working under boost mode.

Pulse signal to switch S2: If MFB produces only U4 then the pulse signals produced by the FLC can be applied to switch S2 to initiate the operation of BDC working under buck mode.

Pulse signal to switch S3: If MFB produces U1 or U2 then the controlled pulses produced by the FLC can be applied to switch S3 to initiate the operation of BDC working under boost mode.
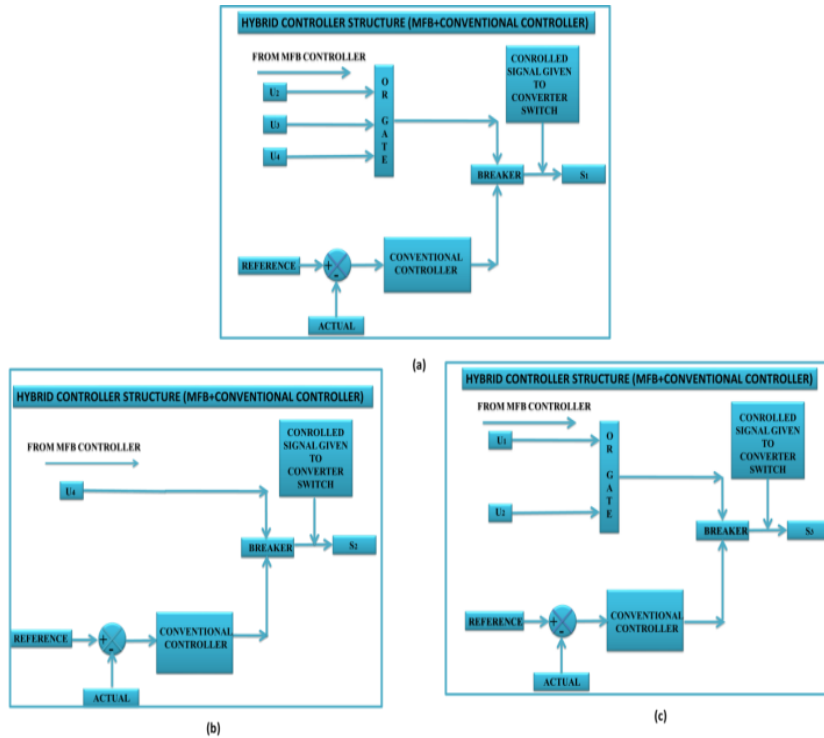

Figure 15. Block diagram representation of converter switches for controlled pulse generation (a) for switch S1 (b) for switch S2 (c) for switch S3

8. Simulation results and discussions

8.1. Mode-I operation results (heavy load condition)

Speed responses of MFB with PID as well as MFB with PI are shown in figure 16. During starting MFB with PID controller speed response has taken 0.9 sec to obtain stable state on another hand MFB with PI has taken 1.7 sec. There are no disturbances present in the both controller's responses after reaching the steady state. At 2 sec a mode corresponding load is applied to the electric motor due to which the speed reduces to less than 4600 rpm, which creates the huge disturbance in both controllers speed responses and the responses are unable to obtain the stable state within specified time period due to heavy load only.

Current responses of MFB with PID and MFB with PI controller are represented in figure 17. Two controller's current responses are subjected to huge variations from starting until the motor reached the steady state. After reaching steady state no fluctuation can be observed in both controllers response. At 2 sec a huge load has been applied to the motor which demands the more current than the rated value. That means during this period more than the rated current required by the motor, which can be supplied by the UC itself. And the motor has not reached the steady state within a given time period due to a heavy load.

Figure 18 represents controlled switching signals produced to the converters by the hybrid controller MFB with PID. During starting of motor requires more power, which can be supplied by the auxiliary source UC, which means the controlled signals are produced to BDC (boost mode). After some time two energy sources combine meets the load requirement up to the stable state, so controlled signals are produced to BDC (boost) as well as UDC (boost). At 0.9 sec motor response reached steady state, which initiates the BDC working as a buck converter and UDC again working as boost converter till load has been applied to the motor. At 2 sec mode corresponding load applied to the electric motor, which initiates the pulse signal generation only to BDC (boost mode). And UC can supply the total transient power required by the electric motor until it reaches the steady state.
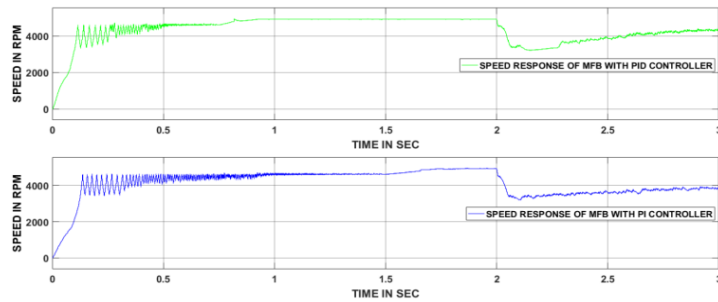

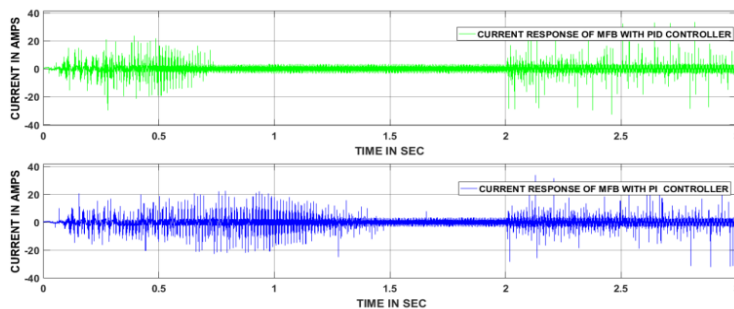Figure 16. Responses corresponding to the speed of the motor

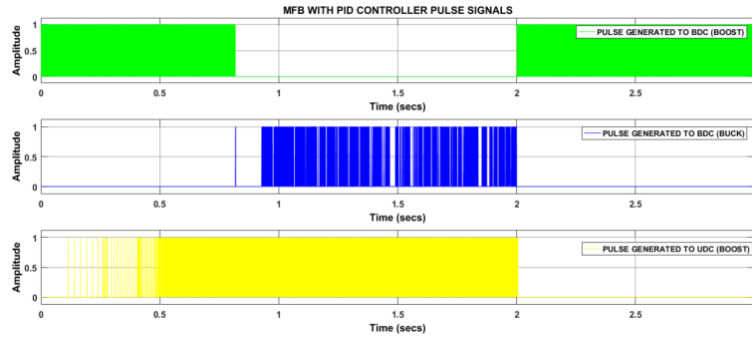Figure 17. Responses corresponding to a current of the motor

Figure 18. Controlled switching signals produced by the MFB plus PID controller to BDC as well as UDC
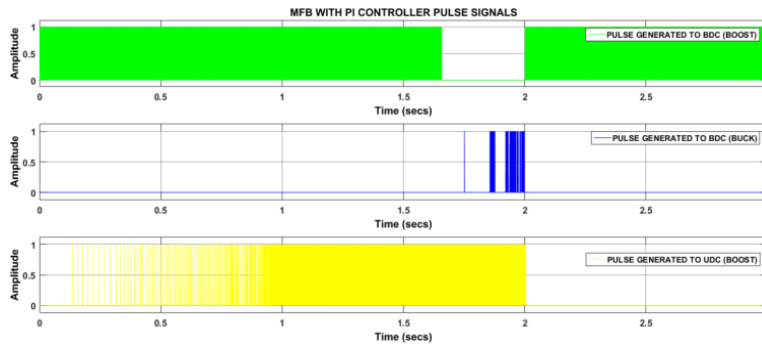

Figure 19. Controlled switching signals produced by the MFB plus PI controller to BDC as well as UDC

Figure 18 represents controlled switching signals produced to the converters by the hybrid controller MFB with PID. During starting of motor requires more power, which can be supplied by the auxiliary source UC, which means the controlled signals are produced to BDC (boost mode). After some time two energy sources combine meets the load requirement up to the stable state, so controlled signals are produced to BDC (boost) as well as UDC (boost). At 1.7 sec motor response reached steady state, which initiates the BDC working as a buck converter and UDC again working as boost converter till load has been applied to the motor. At 2 sec mode corresponding load applied to the electric motor, which initiates the pulse signal generation only to BDC (boost mode). And UC can supply the total transient power required by the electric motor until it reaches the steady state.

8.2. Mode-II operation results (slightly more than rated load condition)

At 2 sec mode corresponding load is applied to the electric motor and the motor speed reduces between 4600 rpm to 4800 rpm, which creates the disturbance in both controllers speed responses. The MFB with PID controller speed response has reached steady within 0.25 sec whereas MFB with PI controller response has taken 0.4 sec to reach the steady state.

Current responses of MFB with PID and MFB with PI controller are represented in figure 21. Two controllers current responses are subjected to huge variations from starting until the motor reached the steady state. After reaching steady state no fluctuation can be observed in both controllers response. At 2 sec mode corresponding load is applied to the motor which demands the slightly more than rated current value. That means during this period slightly more than the rated current required by the motor. And the motor has reached the steady state within a given time period by the hybrid controllers action.
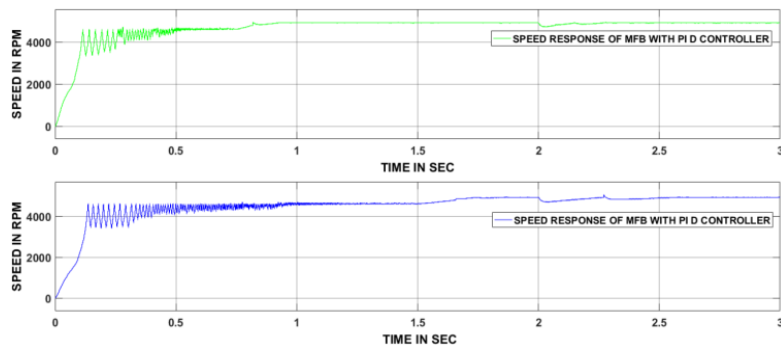

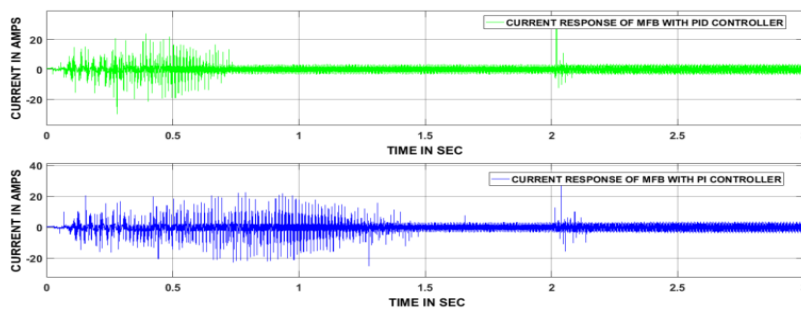*Figure 20. Responses corresponding to the speed of the motor*

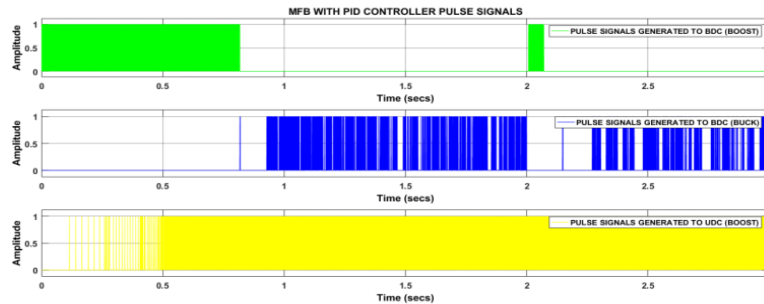*Figure 21. Responses corresponding to current of the motor*

Figure 22. Controlled switching signals produced by the MFB plus PID controller to BDC as well as UDC

At 2 sec mode corresponding load is applied to the electric motor, these initiates the controlled signal production of BDC (boost) as well as UDC (boost). After load applied to the motor total power required by the electric motor can be supplied by the battery as well as UC till it reaches the steady state.
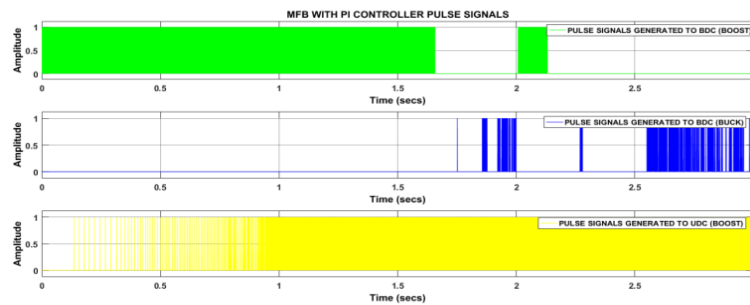

Figure 23. Controlled switching signals produced by the MFB plus PI controller to BDC as well as UDC

8.3. Mode-III operation results (rated load condition)

At 2 sec mode corresponding load is applied to the electric motor and the motor speed reduces between 4801 rpm to 4930 rpm, which creates the small disturbance in both controllers speed responses. The MFB with PID controller speed response has reached steady within 0.15 sec whereas MFB with PI controller response has taken 0.25 sec.

At 2 sec mode corresponding load is applied to the motor which demands the rated current value only. Which means during this period rated current required by the load, which can be given by the battery itself. And the motor has reached the steady state within a given time period by the hybrid controllers action.
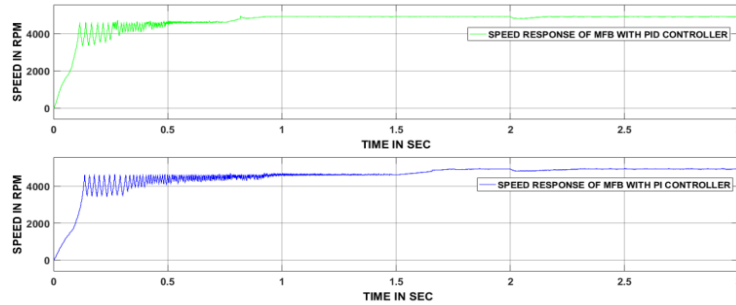
Figure 24. Responses corresponding to speed of the motor

At 2 sec mode corresponding load is applied to the electric motor, these initiates the pulse signal generation only to UDC (boost). After load applied to the motor, no controlled signals are produced to BDC because during rated load condition battery can supply the total power required by the electric motor until it reaches the steady state.
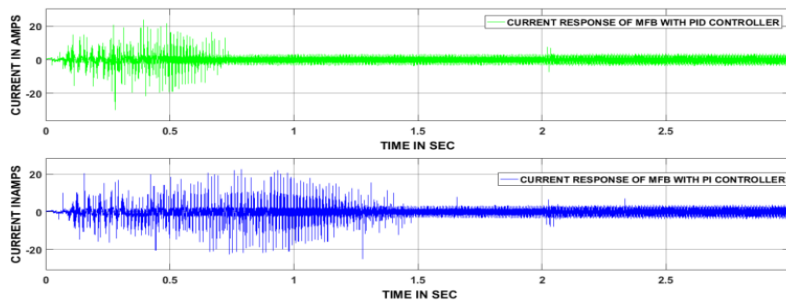

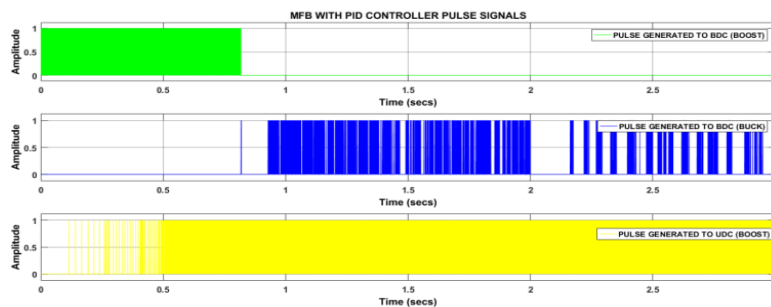*Figure 25. Responses corresponding to current of the motor*

Figure 26. Controlled switching signals produced by the MFB plus PID controller to BDC as well as UDC
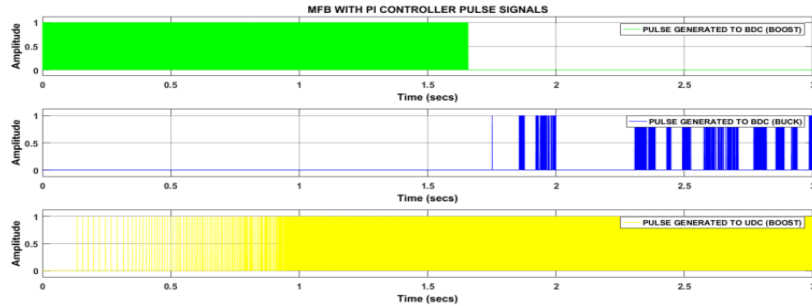
Figure 27. Controlled switching signals produced by the MFB plus PI controller to BDC as well as UDC

8.4. Mode-IV operation results (no load condition)

In this mode of operation, motor speed maintains more than 4931 rpm because during this mode of operation no load is applied to the motor. And UC required power as well motor required power can be supplied by the battery.

Current responses of MFB with PID and MFB with PI controller are represented in figure 29. Two controllers current responses are subjected to huge variations from starting until the motor reached the steady state. After reaching steady state no fluctuation can be observed in both controllers response. During this mode of operation, no load is applied to the electric motor, so no current variations can be observed after 2 sec also.

In this mode of operation, no load is applied to the electric motor so, the controlled switching signals will continue to BDC (buck) and UDC (boost) till load applied to the motor.

Figure 28. Responses corresponding to the speed of the motor
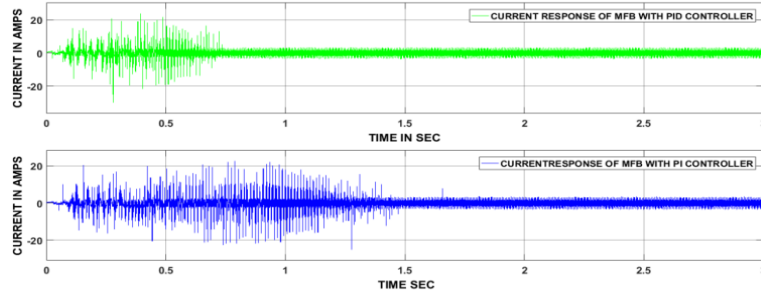
Figure 29. Responses corresponding to a current of the motor

Figure 30. Controlled switching signals produced by the MFB plus PID controller to BDC as well as UDC

Figure 31. Controlled switching signals produced by the MFB plus PI controller to BDC as well as UDC

In this mode of operation, no load is applied to the electric motor so, the controlled switching signals will continue to BDC (buck) and UDC (boost) till load applied to the motor.
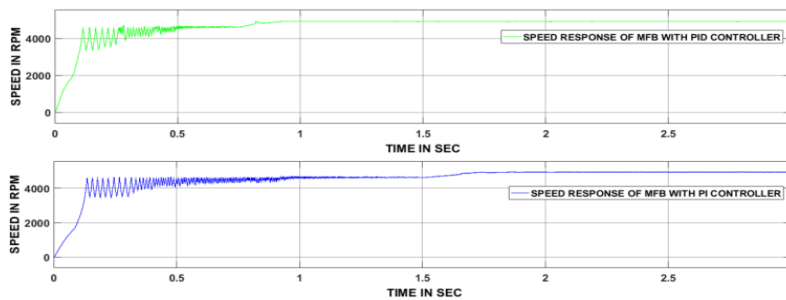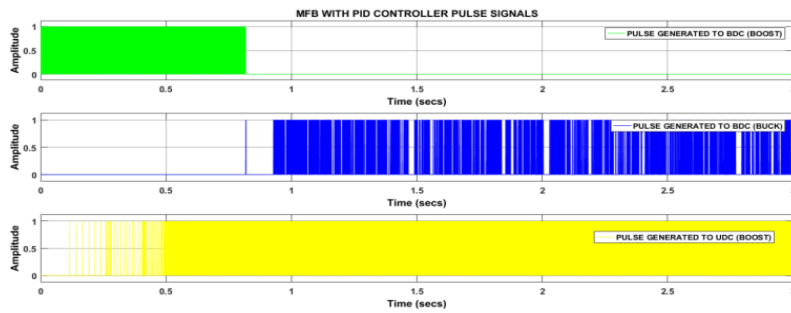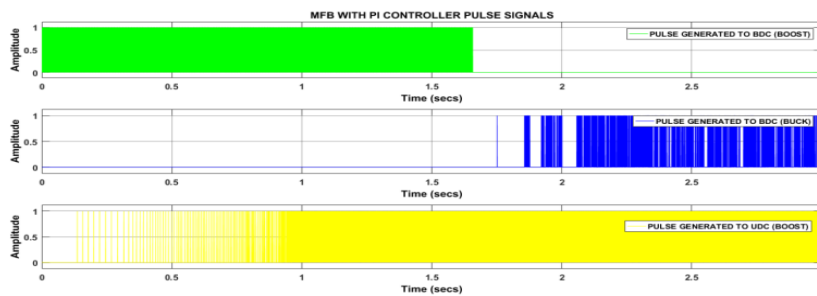
Table 1. DC-DC converters ON/OFF states based on the mode of operation

S.No	Type of mode	State of UDC	State of BDC	Power flow direction
1	Mode-I	Off	Boost	UC supply power to load
2	Mode-II	Boost	Boost	Battery and UC together supply power to Load
3	Mode-III	Boost	Off	Battery only supply power to load
4	Mode-IV	Boost	Buck	The batter can supply power to load as well as UC

Table 2. MFB controller outputs corresponding to speed

S.No	Speed condition associated with mode	ON State Math Function
1	If Speed is ≤4800 rpm	$U_1=1\&U_2=0$, $U_3=0$, $U_4=0$
2	If Speed is from 4600 rpm to 4800 rpm	$U_1=1, U_2=1\& U_3=0$, $U_4=0$,
3	If Speed is from 4801 rpm to 4930 rpm	$U_3=1 \&U_1=0$, $U_2=0$, $U_4=0$
4	If Speed is >4931 rpm	$U_4=1\& U_1=0$, $U_2=0$, $U_3=0$

9. Conclusions

The hybrid controllers (MFB with PID as well as MFB with PI) are designed and implemented to an electric vehicle to switch the energy sources according to the speed of the motor. The designed MFB controller always regulated the switching signals produced by the conventional controllers. Two controllers have given satisfactory results during switching of the battery and UC. The battery gets charged from the solar panel during irradiance and temperature available timings. During mode-I operation MFB controller generated a signal as 1 for only U_1 and 0 for remain U_2, U_3, U_4. During mode-II operation MFB produced a signal as 1 for U_1, U_2 and 0 for remain U_3, U_4. In mode-III operation, MFB produced a signal as 1 for U_3 and 0 for remain math functions. Lastly, in mode-IV operation, MFB produced a signal as 1 for U_4 and 0 for remain math functions. In each and every mode MFB generated signals are compared with pulse signals of a conventional controller, from that final pulse signals are given to particular converter that may be Unidirectional or Bidirectional converter which is purely corresponding to the speed of the motor. The solar power has transferred to the battery as well as the converter directly based on the control switches (CS) action which is connected among the solar panel, battery, and converter. All modes MATLAB/Simulink results including battery charging-discharging are discussed. The comparative analyses of hybrid controllers are tabulated in the conclusion section.

Table 3. Performance of hybrid controllers based on various parameters

Type of Parameter	MFB plus PI	MFB plus PID
Delay time (sec)	0.15	0.1
Rise time (sec)	1.7	0.85
Peak time (sec)	1.8	0.9
Settling time (sec)	1.7	0.9
Maximum peak overshoot (%)	3	2

*Table 4. Comparative analysis of controllers during starting and no load condition
to reach a steady state*

Type of Controller	Controller response time to reach steady with load (sec)	Controller response time to reach steady state at starting (sec)
MFB plus PI	0.3	1.7
MFB plus PID	0.1	0.9

References

Averbukh M., Lineykin S., Kuperman A. (2015). Portable ultracapacitor-based power source for emergency starting of internal combustion engines. *IEEE Transactions on Power Electronics*, Vol. 30, No. 8, pp. 4283-4290. http://dx.doi.org/10.1109/TPEL.2014.2355422

Camara M. B., Gualous H., Gustin F., Berthon A. (2008). Design and new control of DC/DC converters to share energy between supercapacitors and batteries in hybrid vehicles. *IEEE Trans. Vehicular Technology*, Vol. 57, No. 5, pp. 2721-2735. http://dx.doi.org/10.1109/TVT.2008.915491

Cao J., Emadi A. (2012). A new battery/ultracapacitor hybrid energy storage system for electric, hybrid, and plug-in hybrid electric vehicles. *IEEE Transactions on Power Electronics*, Vol. 27, No. 1, pp. 122-132.

Kuperman A., Aharon I. (2011). Battery–ultracapacitor hybrids for pulsed current loads: A review. *Renewable and Sustainable Energy Reviews*, Vol. 15, No. 2, pp. 981-992.

Lustenader E. L., Guess R. H., Richter E., Turnbull F. G. (1977). Development of a hybrid flywheel/battery drive system for electric vehicle applications. *IEEE Transactions on Vehicular Technology*, Vol. 26, No. 2, pp. 135-143. http://dx.doi.org/10.1109/T-VT.1977.23670

Manivannan S., Kaleeswaran E. (2016). Solar powered electric vehicle. *InSustainable Green Buildings and Communities (SGBC), International Conference on 2016 Dec 18, IEEE*, pp. 1-4.

Sadagopan S., Banerji S., Vedula P., Shabin M., Bharatiraja C. (2014). A solar power system for electric vehicles with maximum power point tracking for novel energy sharing. *In India*

Educators' Conference (TIIEC), 2014 Texas Instruments, IEEE, pp. 124-130. http://dx.doi.org/10.1109/TIIEC.2014.029

Shen J., Khaligh A. (2016). Design and real-time controller implementation for a battery-ultracapacitor hybrid energy storage system. *IEEE Transactions on Industrial Informatics*, Vol. 12, No. 5, pp. 1910-1918. http://dx.doi.org/10.1109/TII.2016.2575798

Song Z., Li J., Han X., Xu L., Lu L., Ouyang M., Hofmann H. (2014). Multi-objective optimization of a semi-active battery/supercapacitor energy storage system for electric vehicles. *Applied Energy*, Vol. 13, No. 5, pp. 212-224. http://dx.doi.org/10.1016/j.apenergy.2014.06.087

Tani A., Camara M. B., Dakyo B., Azzouz Y. (2013). DC/DC and DC/AC converters control for hybrid electric vehicles energy management-ultracapacitors and fuel cell. *IEEE Transactions on Industrial Informatics*, Vol. 9, No. 2, pp. 686-696. http://dx.doi.org/10.1109/TII.2012.2225632

Wu D., Todd R., Forsyth A. J. (2015). Adaptive rate-limit control for energy storage systems. *IEEE Transactions on Industrial Electronics*, Vol. 62, No. 7, pp. 4231-4240. http://dx.doi.org/10.1109/TIE.2014.2385043

Xiang C., Wang Y., Hu S., Wang W. (2014). A new topology and control strategy for a hybrid battery-ultracapacitor energy storage system. *Energies*, Vol. 7, No. 5, pp. 2874-2896. http://dx.doi.org/10.3390/en7052874

Yin H., Zhou W., Li M., Ma C., Zhao C. (2016). An adaptive fuzzy logic-based energy management strategy on battery/ultracapacitor hybrid electric vehicles. *IEEE Transactions on Transportation Electrification*, Vol. 2, No. 3, pp. 300-311. http://dx.doi.org/10.1109/TTE.2016.2552721

Zhang J., Shen T. (2015). Energy management strategy design for plug-in hybrid electric vehicles with continuation/GMRES algorithm. *In Control Conference (ECC), 2015 European, IEEE*, pp. 2964-2969. http://dx.doi.org/10.1109/ECC.2015.7330988

Appendix

Appendix A1. Ultracapacitor parameters

Rated capacitance (F)	5
Equivalent DC series resistance (Ohms)	2.1e-3
Rated voltage (V)	6
Number of series capacitors	6
Number of parallel capacitors	1
Operating temperature (Celsius)	25

Appendix A2. Battery parameters

Nominal voltage (V)	6
Rated capacity (Ah)	3.6
Initial state-of-charge (%)	99
Battery response time (s)	10
Fully charged voltage (V)	7.1

Appendix A3. Motor parameters

Rated voltage(V), power(HP), speed (RPM)	12,0.268, 5000
Stator phase resistance Rs (ohm):	1.16/2
Stator phase inductance Ls (H)	194e-6/2
Back EMF flat area (degrees):	120
Inertia, viscous damping, pole pairs, static [J(kg.m^2) F(N.m.s) p()]:	[3.4e-6 1e-7 1]

Appendix A4. Converter parameters

Inductance (H)	300e-3
Capacitance (F)	220e-6
Resistance(ohms)	0.1